Highlights

- The indentation-induced selective etching approach is proposed to fabricate site-controlled pyramidal nanotips on monocrystalline silicon surface.
- The height and radius of the pyramidal nanotips increase with the indentation force or etching time within the etching time of 20 min.
- Various tip arrays on silicon surface can be produced by selective etching of the site-controlled indent patterns, and the maximum height difference of these tips is less than 10 nm.

Site-controlled fabrication of silicon nanotips by indentation-induced selective etching

Chenning Jin[a], Bingjun Yu[a,*], Xiaoxiao Liu[a], Chen Xiao[a], Hongbo Wang[a], Shulan Jiang[a], Jiang Wu[b], Huiyun Liu[b], Linmao Qian[a]

[a] *Tribology Research Institute, Key Laboratory of Advanced Technologies of Materials (Ministry of Education), Southwest Jiaotong University, Chengdu 610031, Sichuan Province, P. R. China*

[b] *Department of Electronic & Electrical Engineering, University College London, Torrington Place, London WC1E 7JE, UK*

** E-mail address: bingjun@swjtu.edu.cn; Tel.: +86 28 87634181; fax: +86 28 87603142.*

ABSTRACT

In the present study, the indentation-induced selective etching approach is proposed to fabricate site-controlled pyramidal nanotips on monocrystalline silicon surface. Without any masks, the site-controlled nanofabrication can be realized by nanoindentation and post etching in potassium hydroxide solution. The effect of indentation froce and etching time on the formation of pyramidal nanotips was investigated. It is found that the height and radius of the pyramidal nanotips increase with the indentation force or etching time, while long-time etching can lead to the collapse of the tips. The formation of pyramidal tips is ascribed to the anisotropic etching of silicon and etching stop of (111) crystal planes in KOH aqueous solution. The capability of this fabrication method was further demonstrated by producing various tip arrays on silicon surface by selective etching of the site-controlled indent patterns, and the maximum height difference of these tips is less than 10 nm. The indentation-induced selective etching provides a new strategy to fabricate well site-controlled tip arrays for multi-probe SPM system, Si nanostructure-based sensors and high-quality information storage.

Keywords: Indentation-induced selective etching; Nanofabrication; Tip array; Silicon

1. Introduction

Nanotechnology has led the boom of information technology and biotechnology, and nanofabrication plays a key role in promoting scientific and technical development in modern world [1-3]. A number of commercial techniques have been developed for fabricating micro/nanoscale structures and devices, and some typical examples include photolithography, electron beam lithography, focused ion beam lithography and so on [4]. Although these prevalent nanofabrication methods got great progress in the past decades, their high operating cost and multiple-step processes largely restrict their applicability in many important areas. None of any current nanofabrication methods can satisfy all aspects of requirements in nanoscience and nanotechnology at the same time for meeting continuous ultra-precision devices and functional diversification [5,6]. To explore new micro/nanofabrication methods with high precision, low cost and high flexibility is still of much concern. Moreover, it is significant to achieve site-controlled nanofabrication on designated surface areas accurately for meeting special requirements [7,8].

In recent years, new methods appear to be flexible alternatives for nanoscale patterning and fabrication. Due to its simplicity, low-cost and flexibility, scanning probe microscope (SPM) showed robust performance in local anodic oxidation [9,10], manipulation of single atoms [11,12], dip-pen nanolithography [4,13], surface texturing [14,15] and so on. As its basic ability, SPM lithography provides a maskless and straightforward approach by mechanical scratching to produce site-controlled nanochannels on the surface of various materials, where mechanical interaction plays a dominant role in the material removal [16,17]. The mechanical scratching can easily result in the wear of a diamond tip [18]. Moreover, the scratch-induced structural damage beneath the nanochannel area, such as amorphization and lattice distortion, cannot be avoided. Such structural damage will degrade the physical and mechanical properties of fabricated nanostructures [19,20]. An alternative SPM-based nanofabrication can be realized by friction-induced selective etching, and protrusive structures or deep grooves can be produced by post etching of a scratch on material surface, such as silicon, quartz, glass and so on [21-23]. For producing protrusive nanostructures, the amorphous layer and/or deformed crystal layer beneath the scratched area can act as an etching mask in KOH aqueous solution [24-26]. In contrast, the scratched area after tribochemical removal of surface oxide can promote the chemical attack from the etching solutions and result in deep groove [27]. It is also noted that high-aspect nanostructures can be produced on monocrystalline silicon through friction-induced selective etching of a scratched Si_3N_4 mask [28]. Various patterns, including slopes and hierarchical stages, can be

produced by programming the loading mode and scanning traces. The friction-induced selective etching provides an active way for site-controlled nanofabrication without any masks.

Since the nanoindentation can lead to a series of crystal transformation beneath the contact area [29], the pressed area is expected to act as a mask in post etching. In the present study, a simple nanofabrication method through indentation-induced selective etching was established to prepare pyramidal nanotips on silicon surface. The effect of indentation force and etching time on the formation of pyramidal tips was investigated, and the fabrication mechanism was addressed. As a maskless and straightforward nanofabrication approach, the indentation-induced method provides a new strategy to fabricate well site-controlled nanoscale tip-arrays and high-density storage structure.

2. Materials and Methods

2.1. Materials

The Si(100), Si(110) and Si(111) wafers were purchased from MEMC Electronic Materials, Inc., USA. By an atomic force microscope (AFM; SPI3800N, Seiko Instruments Inc., Japan), the surface root-mean-square (RMS) roughness of the silicon wafers was measured as no more than 0.1 nm over a 1 μm × 1 μm area. To eliminate the effect of the native oxide layer on the fabrication, silicon wafers were dipped in 5 wt.% HF solution for 2 minute to etch off the oxide layer [27]. Then the samples were ultrasonically cleaned with acetone, ethanol and deionized water for 3 min in turn to remove surface contaminations.

2.2. Fabrication methods

As shown in Fig. 1, the fabrication process consists of nano-indentation and post etching. With a Berkovich tip and an in-situ nanomechanical test system (TI900, Hysitron Inc., USA), a series of patterned indents were produced on silicon surface under various applied normal loads F_n of 2, 3 and 4 mN (Fig. 1a). Then the indented surface was immersed in KOH aqueous solution for various etching time, and pyramidal nanotips were produced in-situ from the indentation area on silicon surface (Fig. 1b). A mixture of 20 wt.% KOH solution and isopropanol alcohol (IPA) with the volume ratio of 5:1 was used as an etchant for selective etching, and IPA was employed to improve the surface quality [27]. The temperature for the selective etching was set as $25^oC \pm 0.5^oC$. All AFM images of the fabricated nanostructures on silicon surface were scanned by a Si_3N_4 tip (MLCT, Veeco Instruments Inc., USA) in vacuum

with a nominal tip radius of ~20 nm.

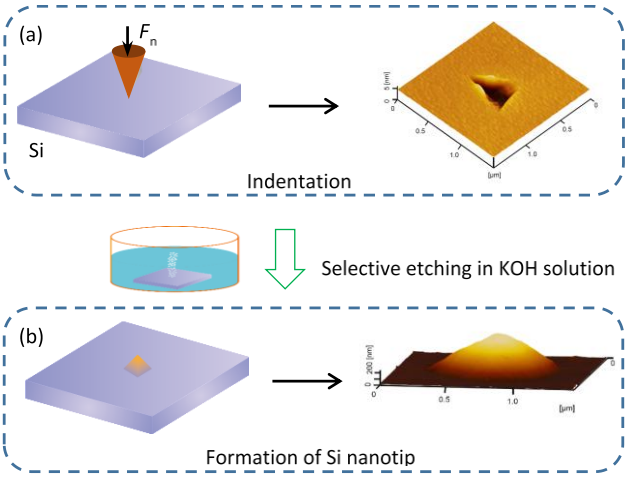

Fig. 1. Schematic diagram for the fabrication process by the indentation-induced selective etching. (a) Schematic diagram and AFM image of an indent produced on Si surface under an indentation force F_n. (b) A pyramidal tip created on Si surface after selective etching in KOH aqueous solution.

3. Results and discussions

3.1. Effect of etching time on indentation-induced selective etching

The etching time has a strong effect on the formation of pyramidal nanotips during indentation-induced selective etching. An indent with a depth of about 6 nm was firstly produced by indenting under F_n=2 mN. Then a pyramidal nanostructure was detected on the indent area after dipping in KOH aqueous solution, as shown in Fig. 2. It was noted that the formation of nanotips was obviously etching time-dependent, and the height of the nanostructure increased firstly and then decreased with increasing etching time. The protrusive nanotips almost collapsed completely after etching for 60 min. The variation of the height of these nanotips with etching time was plotted in Fig. 3. The height increased from -6 to 280 nm with the increase in etching time from 0 to 20 min, and 20 min-etching led to a maximum height. Since the deformation layer beneath the indented area can be etched away gradually with the increase in the etch time [25]. Long-time etching can also cause the etch-off of the deformation layer, and then the selective etching becomes weak and the protrusive structures trend to disappear completely. For example, the height after etching for 60 min was ~2 nm, and it is comparable with the height of surface asperities.

Fig. 3 shows the radii of the pyramidal tips plotted as a function of the etching time,

which is similar to the trend of change in the height. When the sample was etched for 25 min, the radius reaches ~300 nm. Considering that the height and radius of pyramidal nanostructure increase linearly with the etching time, the etching from 5 to 20 min is better for a controllable fabrication.

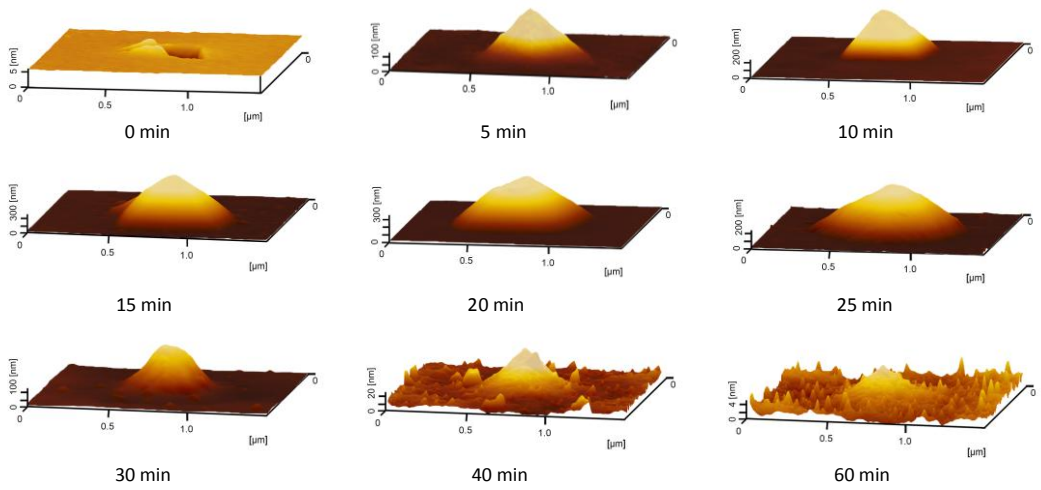

Fig. 2. Indentation-induced selective etching under various etching time. The indentation force for the indentation is 2 mN.

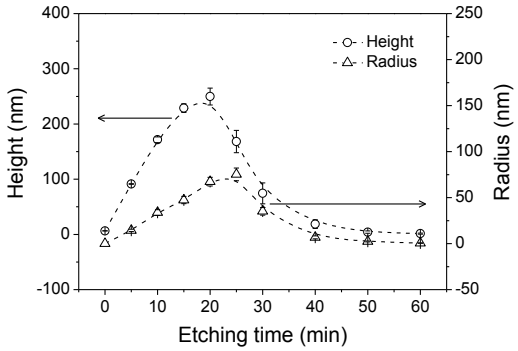

Fig. 3. The height (left) and radius (right) of the nanotips as a function of etching time.

3.2. Effect of indentation force on indentation-induced selective etching

In addition to the etching time, the indentation force also reveals a great effect on the indentation-induced selective etching. Since the etching time of 20 min can lead to the maximum growth of the pyramidal nanotips in the present study, the etching time of 20 min will be used for the following comparative test. As shown in Fig. 4a, indentation tests were performed on Si surface under various loads of 2, 3 and 4 mN, and the depth of the indents increased with the normal load. Fig. 4b shows the AFM images of the sample after etching in

KOH aqueous solution for 20 min. The height and radius of the pyramidal nanostructure increased with the normal load during etching. At a load of 2 mN, the height and radius of the tip structure are 280 nm and 100 nm, while at a load of 4 mN, the height and radius are 480 and 300 nm, respectively. Therefore, low applied normal load in scratching can facilitate the formation of sharp tip structure.

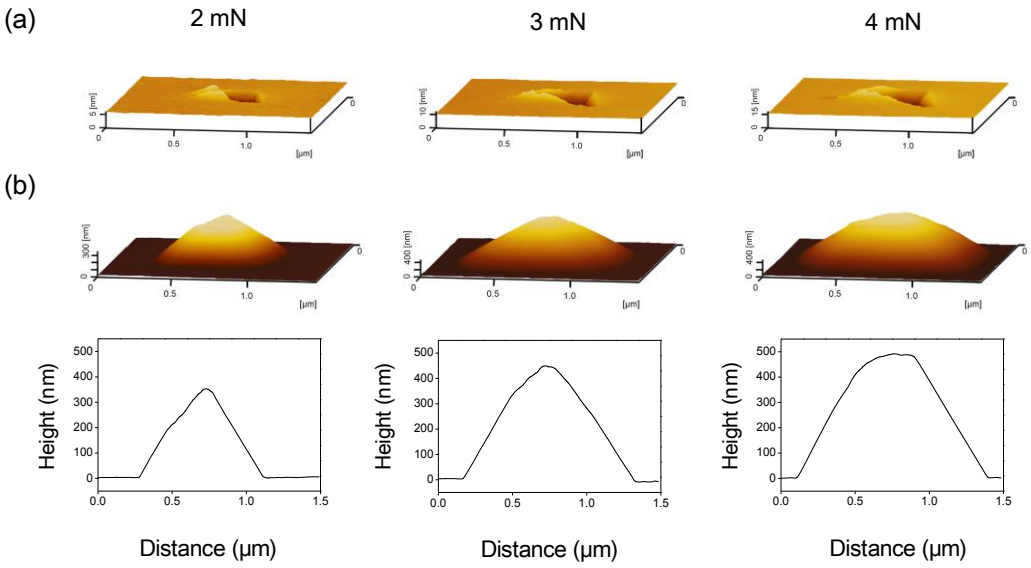

Fig. 4. Indentation-induced nanofabrication under various applied indentation force. (a) AFM images of the indents created on Si surface under 2, 3 and 4 mN. (b) AFM images of the pyramidal nanotips after etching for 20 min. The cross-section profiles across tip peaks were plotted below for the comparison.

3.3. Mechanism of indentation-induced selective etching

The fabrication mechanism could be related to the different etching rate of the indentation area and original silicon surface, and the indent area triggers the selective etching. In the friction-induced selective etching process, the residual amorphous and deformed silicon layer produced by tip scratching can be directly used as an etching mask in KOH solution to fabricate protrusive nanostructures [24,25]. The amorphous and crystal transformation were also founded beneath the indented area [29]. It is deduced that in this study the crystal deformation beneath the indented area on Si surface could also act as a resist mask against etching, and the formation of the inclined planes in the pyramidal structure is ascribed to the anisotropic etching of Si crystal planes in KOH aqueous solution. The indentation-induced crystal deformation, including amorphous layer and multiple phases of silicon crystal, can hinder the etching, resulting in a quite lower etching rate of the indent than the unprocessed

silicon surface. With the onset of selective etching, different crystal planes are exposed to the etching solution around the indenter tip-affected area. The etching rate of other crystal planes of silicon, such as (100) and (110), is much higher than that of (111) plane [30,31]. Therefore, the (111) crystal plane can act a barrier to resist the etching, forming pyramidal planes, as shown in Fig. 5. The inclined pyramidal plane is exactly the etch-stop surface of (111) crystal plane [24,32]. It is noted that the slope angle of the inclined plane in the present study is about 55° (close to the included angle of (100) and (111) crystal planes), by which the above mechanism for selective etching can be verified.

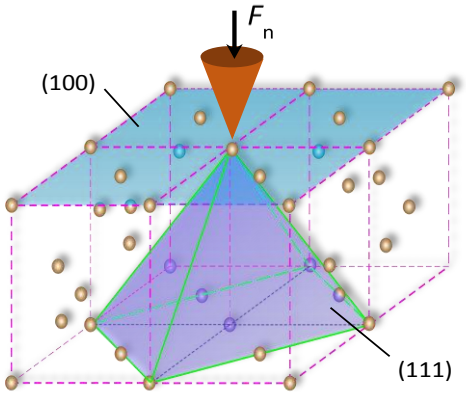

Fig. 5. The schematic illustration for the selective etching of an indent on Si(100).

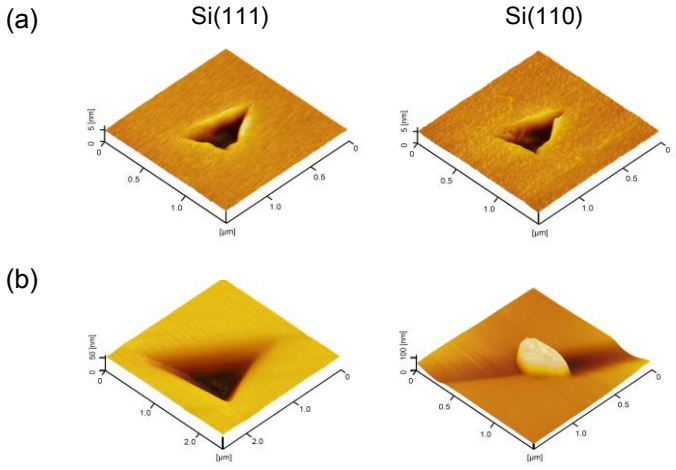

Fig. 6. Indentation-induced selective etching on Si(111) and Si(110) substrates. (a) AFM images of the indentation array created on Si(111) and Si(110) surface under the indentation force of 2 mN. (b) AFM images of the indents after etching for 10 min.

For comparison, the indentation-induced nanofabrication was also conducted on Si(111) and Si(110) surface. As shown in Fig. 6, the crystal plane has an obvious effect on the

indentation-induced selective etching process. After the selective etching, deeper holes were detected from the indents on Si(111), while protrusive structures were created on Si(110). For the (111) crystal plane with a very low etching rate, the crystal deformation in the indentation can promoting the etching rather than acting as a mask. In other words, Si(100) substrate is the right candidate for realizing the proposed indentation-induced selective etching to fabricate pyramidal nanotips.

3.4. Nanotip arrays fabricated on Si(100) by indentation-induced selective etching

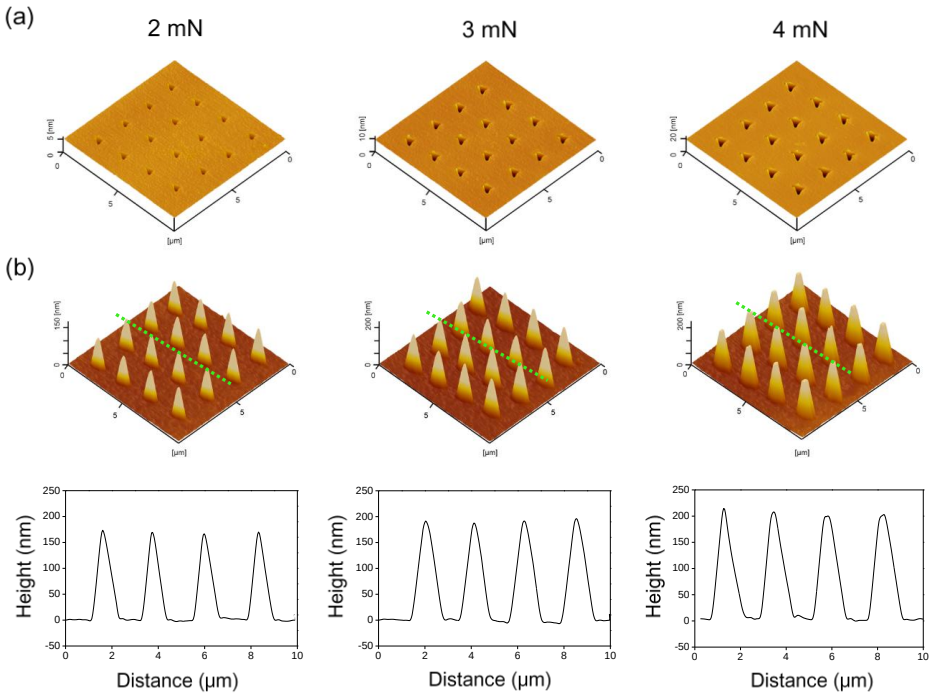

Fig. 7. Pyramid-shaped tip arrays fabricated on Si(100) surface by indentation-induced selective etching. (a) AFM images of the indents on silicon produced at indentation force of 2, 3 and 4 mN. (b) Pyramidal tip arrays by selective etching of the indents in (a) for 10 min. The cross-section profiles of the tips were obtained from the dotted lines marked in (b).

With the indentation-induced selective etching nanofabrication method, a series of pyramid-shaped tip arrays were fabricated on Si(100) surface. Fig. 7a illustrates the 4 × 4 indentation arrays on silicon produced at indentation force of 2, 3 and 4 mN. The tip arrays were fabricated after selective etching of the indents in KOH aqueous solution for 10 min (Fig. 7b), and the corresponding profiles of these tips were measured and plotted. It is noted that the maximum height difference of the tips after selective etching of the indents created under 2 mN is less than 10 nm, showing a good repeatability of the proposed fabrication method. By

designing the configuration of the indentation pattern, various tip arrays can be produced by the proposed fabrication method.

When the indentation-induced selective etching method is used, long etching time in KOH aqueous solution could cause the roughness of Si surface [25]. For a tip array production, it is necessary to ensure that the tip is quite higher than the asperities around. Therefore, it is necessary to investigate the asperities on the rough surface resulting from etching. The maximum height of surface asperities with the etching time ranging from 0 to 60 min is plotted in Fig. 8, and AFM images of some surface asperities are shown in the inset. When Si sample is etched from 0 to 40 min, the height of asperities is less than 10 nm, which is quite lower than the produced tip arrays. However, when the etching time is increased to 60 min, the asperity height can be up to 20 nm, which is comparable with the collapsed tips (Fig. 2). Therefore, combining the results in Fig. 3, the etching time no more than 20 min is recommended for indentation-induced selective etching to fabricate the uniform tip arrays.

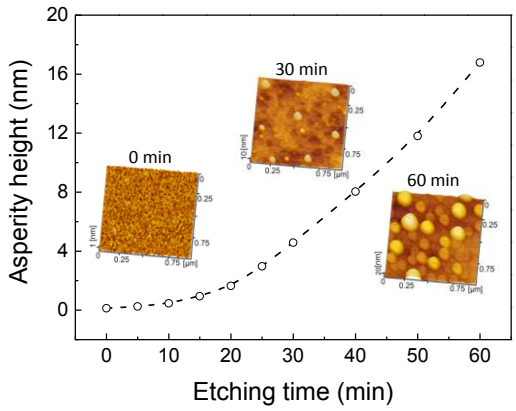

Fig. 8. The maximum height of surface asperities on Si over an area of 1 μm × 1 μm plotted as a function of etching time. The inset picture shows the AFM images after different etching time.

Summarily, without any resist mask and template, site-controlled nanofabrication can be realized on Si(100) surface through indentation-induced selective etching. This method provides meaningful strategy for the application of multiple-tip SPM and high-density information storage. SPM-based lithography has yet been rarely used in the field of industrial manufacturing, because of its disadvantages of small scanning range and low efficiency, and a nice bit of research has been focused on developing multi-probe SPM [33,34]. To produce tip arrays is significant for a multi-probe SPM system, where the multi-tip arrays play a key role in realizing large-scale and high efficiency scanning [35,36]. Even with impressive recent

advances in cantilever array design, those arrays tend to be highly special for a given application and is quite expensive [37]. In contrast, the tip-array fabrication by the indentation-induced selective etching in the present study is of low cost and environmentally friendly, and can be easily realized. In addition, the indentation-induced selective etching provides new strategy for fabricating Si nanostructure-based sensors [38], and high-quality MEMS-based scanning-probe data-storage system [39,40].

4. Conclusion

In summary, we have proposed a simple nanofabrication approach by indentation-induced selective etching, and pyramid-shaped tip arrays can be produced on Si(100) surface. The height and radius of the tip produced are dependent on the indentation force during tip pressing process and the etching time in KOH aqueous solution. The formation of pyramidal planes is ascribed to the anisotropic etching of Si crystal planes in KOH aqueous solution. The indent area triggers the selective etching, and (111) plane can stop the etching to some extent, resulting in the formation of pyramidal tips. As a maskless and straightforward nanofabrication method, the indentation-induced selective etching nanofabrication provides a new strategy to produce well site-controlled tip arrays for multi-probe SPM system and high-density information storage.

Acknowledgements

The authors are grateful for the support by the Natural Science Foundation of China (51305365 and 51605400) and the Fundamental Research Funds for the Central Universities (2682015CX037).

References

[1] F. Priolo, T. Gregorkiewicz, M. Galli, T.F. Krauss, Silicon nanostructures for photonics and photovoltaics, Nat. Nanotechnol. 9 (2014) 19–32.
[2] A.D. Stroock, S.K.W. Dertinger, A. Ajdari, I. Mezić, H.A. Stone, G.M. Whitesides, Chaotic mixer for microchannels, Science 295 (2002) 647–651.
[3] J.M. Perry, K. Zhou, Z.D. Harms, S.C. Jacobson, Ion transport in nanofluidic funnels, ACS Nano 4 (2010) 3897–3902.
[4] A.S. Wee, Selected topics in nanoscience and nanotechnology, World Scientific, Singapore, 2009.
[5] Y. Wang, X. Hong, J. Zeng, B. Liu, B. Guo, H. Yan, AFM Tip Hammering Nanolithography, Small 5 (2009) 477–483.
[6] S. Chou, C. Keimel, J. Gu, Ultrafast and direct imprint of nanostructures in silicon, Nature 417 (2002) 835–837.
[7] Z. Cui, Nanofabrication: Principles, capabilities and limits, Springer, Germany, 2008.
[8] R. Luttge, Nano- and microfabrication for industrial and biomedical applications (2nd Edition), William Andrew Elsevier, 2016.
[9] D. Stiévenard, B. Legrand, Silicon surface nano-oxidation using scanning probe microscopy,

Prog. Surf. Sci. 81 (2006) 112–140.
[10] X.N. Xie, H.J. Chung, C.H. Sow, A.T.S Wee, Nanoscale materials patterning and engineering by atomic force microscopy nanolithography, Mater. Sci. Eng. R. 54 (2006) 1–48.
[11] D.M. Eigler, E.K. Schweizer, Positioning single atoms with a scanning tunneling microscope, Nature 344 (1990) 524–526.
[12] H.C. Manoharan, C.P. Lutz, D.M. Eigler, Quantum mirages formed by coherent projection of electronic structure, Nature 403 (2000) 512–515.
[13] R.D. Piner, J. Zhu, F. Xu, S. Hong, C.A. Mirkin, "Dip-Pen" Nanolithography, Science 283 (1999) 661–663.
[14] D. Pires, J.L. Hedrick, A.D. Silva, J. Frommer, B. Gotsmann, H. Wolf, M. Despont, U. Duerig, A.W. Knoll, Nanoscale three-dimensional patterning of molecular resists by scanning probes, Science 328 (2010) 732–735.
[15] R. Garcia, A.W. Knoll, E. Riedo, Advanced scanning probe lithography, Nat. nanotechnol. 9 (2014) 577–587.
[16] Y. Yan, Z. Hu, X. Zhao, T. Sun, S. Dong, X. Li, Top-down nanomechanical machining of three-dimensional nanostructures by atomic force microscopy, Small 6 (2010) 724–728.
[17] B. Yu, H. Dong, L. Qian, Y. Chen, J. Yu, Z. Zhou, Friction-induced nanofabrication on monocrystalline silicon, Nanotechnology 20 (2009) 465303.
[18] M. Bai, K. Kato, N. Umehara, Y. Miyake, J. Xu, H. Tokisue, Scratch-wear resistance of nanoscale super thin carbon nitride overcoat evaluated by AFM with a diamond tip, Surf. Coat. Tech. 126 (2000) 181–194.
[19] P.J. Zanzucchi, M.T. Duffy, Surface damage and the optical reflectance of single-crystal silicon, Appl. Optics. 17 (1978) 3477–3481.
[20] B. Yu, X. Li, H. Dong and L. Qian, Mechanical performance of friction-induced protrusive nanostructures on monocrystalline silicon and quartz, Micro Nano Lett. 7 (2012) 1270–1273.
[21] J. Guo, C. Song, X. Li, B. Yu, H. Dong, L. Qian, Z. Zhou, Fabrication mechanism of friction-induced selective etching on Si(100) surface, Nanoscale Res. Lett. 7 (2012) 152.
[22] C. Song, X. Li, S. Cui, H. Dong, B. Yu, L. Qian, Maskless and low-destructive nanofabrication on quartz by friction-induced selective etching, Nanoscale Res. Lett. 8 (2013) 140.
[23] C. Song, B. Yu, M. Wang, L. Qian, Rapid and maskless nanopatterning of aluminosilicate glass surface via friction-induced selective etching in HF solution, RSC Adv. 97 (2015) 79964–79968.
[24] J. Guo, C. Song, X. Li, B. Yu, H. Dong, L. Qian, Z. Zhou, Fabrication mechanism of friction-induced selective etching on Si(100) surface, Nanoscale Res. Lett. 7 (2012) 152.
[25] C. Jin, B. Yu, C. Xiao, L. Chen, L. Qian, Temperature-dependent nanofabrication on silicon by friction-induced selective etching, Nanoscale Res. Lett. 11 (2016) 229.
[26] J. Guo, C. Xiao, B. Peng, L. Qian, Tribochemistry-induced direct fabrication of nondestructive nanochannels on silicon surface, RSC Adv. 5 (2015) 100769–100774.
[27] J. Guo, B. Yu, L. Chen, L. Qian, Nondestructive nanofabrication on Si(100) surface by tribochemistry-induced selective etching, Sci. Rep. 5 (2015) 16472.
[28] J. Guo, B. Yu, X. Wang, L. Qian, Nanofabrication on monocrystalline silicon through friction-induced selective etching of Si_3N_4 mask, Nanoscale Res. Lett. 9 (2014) 241.
[29] J. Jang, M.J. Lance, S. Wen, T.Y. Tsui, G.M. Pharr, Indentation-induced phase transformations in silicon: influences of load, rate and indenter angle on the transformation behavior, Acta Mater. 53 (2005) 1759–1770.
[30] M. Shikida, K. Sato, K. Tokoro, D. Uchikawa, Differences in anisotropic etching properties of KOH and TMAH solutions, Sensor. Actuat. A-Phys. 80 (2000) 179–188.
[31] H. Seidel, L. Csepregi, A. Heuberger, H. Baumgärtel, Anisotropic etching of crystalline silicon in alkaline solutions I. Orientation dependence and behavior of passivation layers, J Electrochem. Soc. 137 (1990) 3612–3626.
[32] F. Ebrahimi, L. Kalwani, Fracture anisotropy in silicon single crystal, Mat. Sci. Eng. A 268 (1999) 116–126.
[33] E. Albisetti, D. Petti, M. Pancaldi, M. Madami, S. Tacchi, J. Curtis, W. King, A. Papp, G. Csaba, W. Porod, Nanopatterning reconfigurable magnetic landscapes via thermally assisted scanning probe lithography, Nat. Nanotechnol. 11 (2016) 545–551.
[34] J.S. Lee, J. Song, S.O. Kim, S. Kim, W. Lee, J.A. Jackman, D. Kim, N.J. Cho, J. Lee,

Multifunctional hydrogel nano-probes for atomic force microscopy, Nat. Commun. 7 (2016) 11566.
[35] T. Nakayama, O. Kubo, Y. Shingaya, S. Higuchi, T. Hasegawa, C.S. Jiang, T. Okuda, Y. Kuwahara, K. Takami and M. Aono, Development and application of multiple-probe scanning probe microscopes, Adv. Mater. 24 (2012) 1675–1692.
[36] M. Zhang, D. Bullen, S.W. Chung, S. Hong, K.S. Ryu, Z.F. Fan, C.A. Mirkin, C. Liu, MEMS nanoplotter with high-density parallel dip-pen nanolithography probe arrays, Nanotechnology 13 (2012) 212–217.
[37] W. Shim, A.B. Braunschweig, X. Liao, Hard-tip, soft-spring lithography, Nature 469 (2011) 516–520.
[38] W. Li, M. Hu, P. Ge, J. Wang, Y. Guo, Humidity sensing properties of morphology-controlled orderedsilicon nanopillar, Appl. Surf. Sci. 317 (2014) 970–973.
[39] F.E. Kalff, M.P. Rebergen, E. Fahrenfort, J. Girovsky, R. Toskovic, J.L. Lado, J. Fernández-Rossier, A.F. Otte, A kilobyte rewritable atomic memory, Nat. Nanotechnol. 11 (2016) 926–929.
[40] T. Kaule, Y. Zhang, S. Emmerling, S. Pihan, R. Foerch, J. Gutmann, H-J. Butt, R. Berger, U. Duerig, A.W. Knoll, Nanoscale Thermomechanics of Wear-Resilient Polymeric Bilayer Systems, ACS Nano 7 (2013) 748–759.